profiles along the horizontal line between the simulation and experiment. The two profiles have high correlation in terms of temperature distribution pattern. The bigger temperature rise in and around the nanoparticle populated insert is clearly seen in both simulation and experimental temperature maps. It was also observed that the average temperature difference of 3 °C inside and outside the insert in the temperature map well coincides with the one measured with the optic fiber sensor.
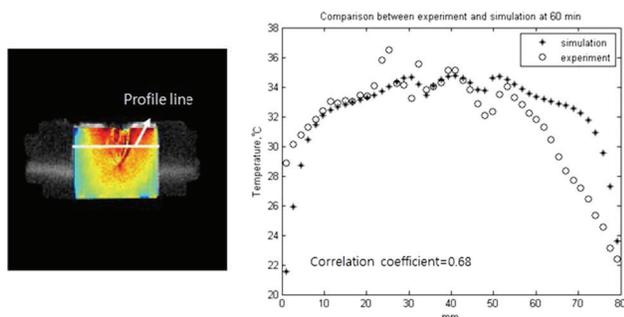
Fig. 2 The MRI image of the phantom (*left*) and temperature profiles along the red line (*right*) obtained by FDTD simulation and experiment

Conclusions

The experiment has shown that nanoparticle-mediated capacitive hyperthermia can induce focused temperature rise at the nanoparticle-populated region. MRI temperature mapping will be very useful for temperature monitoring in nanoparticle-mediated RF capacitive hyperthermia in which accurate temperature monitoring is critical.

Geant4-based framework for hadronic radiotherapy simulations

A.N. Solovev[1], U.A. Stepanova[1], S.E. Uliyanenko[1], A.E. Chernukha[1], V.V. Fedorov[1]
[1]A. Cyb Scientific Research Centre of Radiology of the Hertsen Federal Medical Research Centre of the Ministry of Health of the Russian Federation, Obninsk, Russia

Keywords Monte-Carlo method · Hadron therapy · Radiation treatment planning · Geant4

Purpose

Hadron therapy is an external beam radiotherapy for oncology radiation treatment. The main advantage of hadron therapy is essential physical properties of such particles. On the other hand, there are many challenges while implementing and using such particles in real treatment case. That is why we must accurately simulate hadronic interactions with attendant electromagnetic physics before patient treatment and even before biophysics experiments.

Geant4 is a commonly known framework for "the simulation of the passage of particles through matter: but such simulations cannot be done without understanding how specific physics model will work. Another problem is that switching between physic models usually requires recompilation of users program. In this work we provide a functional open-source framework on the top of Geant4 to simplify user code design and usage as a base for future study.

Methods

The principle development idea was following: our code should always work with the latest Geant4 version and should not modify original Geant4 classes. We used python 2.7.9 for making interactive GUI to simplify running Geant4 programs with parameterization and boost 1.55 inside our C++ user code. As the organizational concept we tried to range which features are most important and should be

implemented first and how we can optimize current simulation methods in terms of simulation speed and accuracy.

Results

We implemented several features which don't exist in original Geant4, such as:

- exit by simulation time condition;
- run simulation till statistical error detector doesn't exceed certain value, supporting simple and voxel detectors, extending G4MultiFunctionalDetector and for all our detectors;
- continuation run with saving state of all detectors, including classes over standard G4AnalysisManager;
- scoring dE/dx values and it's statistics;
- several complex detector classes for effective dose scoring with spectrum parameters;
- JSON-based input files for fine tuning of hadronic physics models, pretty similar to GATE (another Geant4 framework made by OpenGATE collaboration) solution, but using another format. Still we don't provide such files for electromagnetic physics but option list to choose from standard electromagnetic interaction models;
- MCNP lattice format reader and converter to Geant4 nested phantom parametrization model, including voxel structure and materials builder;
- Extendable command-line parser;
- Python GUI interface for running Geant4 simulations with database and network run manager.

All our code supports native Geant4 multithreading mechanism.

The framework was used during experimental study on neutron beam facility with neutron generator NG-24 14.5 ± 1 MeV performed at MRRC, Obninsk, Russia. It allows us to optimize simulation tasks, e.g. assess absorbed dose at tissue-equivalent target with and without proton balance as well as turn off some unnecessary interactions for this task. Using this framework allows us to select appropriate physics models that leads us to speeding up simulation up to 40 % comparing to standard FTFP_BERT_HP/QGSP_BIC_HP model saving the simulation accuracy.

Also we used our framework for dosimetric biophysics study at cyclotron carbon ion 5.4 GeV beam at U-70 particle accelerator at IHEP, Protvino, Russia. The results of this study will be available soon but we can confirm that our simulation results are in a good agreement with measured experimental data. The framework was used both before the experiments to calculate initial setup parameters and positions of Bragg peak and after experiments to verify and confirm measured control values.

Conclusions

We provide a functional open-source Geant4 based framework for expanding user experience with Geant4. We intend to use it as a part of the fast neutron treatment planning system now under development at MRRC, Obninsk, Russia and for our forthcoming studies with proton and carbon beams. It could also be useful for simulation low-level radiation effects for DNA damage with Auger electrons and cell damage with free radicals and for our long-term study of principles of hadron damage on living cells. We are welcome for your feedback. The source code is available at bitbucket.org/mrrc/npplan under LGPL license.

A new workflow for image guided intraoperative radiotherapy using fluoroscopy based pose tracking

S.S. Goswami[1], J.E. Ortuño Fisac[1], G. Wollny[1], V. García-Vázquez[2], E. Marinetto[2], A. Santos Lleó[1], J. Pascau[2], M.J. Ledesma Carbayo[1]
[1]Universidad Politécnica de Madrid, Madrid, Spain;
[2]Universidad Carlos III de Madrid - Hospital General Universitario Gregorio Marañón, Madrid, Spain

Keywords IOERT · Registration · 2D–3D · Surgery planning · Intensity based registration

Purpose

Intraoperative electron beam radiation therapy (IOERT) involves the radiation delivery to the postresected tumor bed during the surgical procedure. Surgical and radiation therapy planning use preoperative CT data mimicking the patient pose during the intervention. However, patient placement and anatomy modifications during the actual procedure could differentiate significantly from the pre-operative situation, and consequently a planning update would be necessary. Due to the difficulty to acquire conventional CT scans at the time of the surgical intervention, several strategies have been proposed. Optical tracking systems have been used to track the treatment applicator pose [1], but these external based tracking methods require calibration, present limitations related with the tracker size and/or line-of-sight, and do not provide information from internal structures. Alternative volumetric imaging devices like cone-beam CT could be used and are under investigation, however there availability is limited.

In this work we propose the use of 2D fluoroscopy by C-arm as intraoperative source of information, as it is the most common imaging modality that is used in surgical rooms. With the premise that a suitable tracking system should minimize the use of additional calibration procedures or external tracking devices, the proposed workflow uses an applicator with markers, skin markers and the fluoroscopy projections, adding the capability of locating the applicator with respect to the internal anatomy of the region of interest.

In this context, the objective of this work is to propose a workflow to calculate the relative pose of the treatment applicator and its relation with the internal structures. The workflow includes different steps including the pose estimation of the C-arm, the registration between intra-operative C-arm projection images and a pre-operative CT volume image and finally positioning the virtual applicator accurately in the pre-operative volume for planning and verification of IOERT treatment.

Methods

The position of the virtual applicator in the pre-operative CT scan is estimated in a three stage workflow that involves: the radiation therapy applicator with a marker pattern by construction, the preoperative CT of the patient with skin markers around the surgery incision area, and the C-arm projections with the applicator located in the treatment position (Fig. 1). Given this data the following steps are followed:

1. Estimation of the rigid transformation between the C-arm camera and the applicator. The position and orientation of the C-arm in the applicator reference frame are determined from 2D–3D point correspondences using the applicator markers. These are segmented using a difference of Gaussians (DoG) blob detector in scale-space, with contrast, aspect ratio and range of scale as discriminating parameters. We compute four solutions for the absolute pose using three 2D-to-3D correspondences [2] and a Random Sample Consensus (RANSAC) outlier-rejection step.

2. Estimation of an initial rigid transformation between the applicator and the CT preoperative data. Once the C-arm projection poses are estimated, the second stage can be solved with a 3D–3D point-based rigid registration algorithm using 3D surface skin markers and their projections on the intra-operative projection images.

3. Refinement using a 3D–2D intensity based registration. Taking into account that the surgical procedure alters the anatomy a refinement process based on 3D–2D intensity-based registration is necessary to accurately align the internal structures. This 3D–2D intensity based registration process considers normalized mutual information (NMI) as the similarity measure and a simplex optimization. The Digitally Reconstructed radiographs (DRR) are calculated for only those rays that pass through the whole length of the volume, increasing the probability of getting better registration results and avoids computational overhead. We have considered the portion of the fluoroscopy image which is equal to the portion of image plane considered as DRR. Both images are scaled to the same intensity range.

As a proof of concept, the proposed workflow was used with a low-cost phantom reproducing all the steps that would be involved in a real case. The phantom consisted on a plastic bone surrounded by cylindrical foam. Fourteen metallic nipple markers (diameter 1 mm) were located on the surface in 4 predefined constellations of different number of markers (5, 4, 3, 2) around the region of interest and another 12 markers of 2 mm diameter were placed on the applicator (diameter 10 cm) in a spiral order. The pre-operative CT ($512 \times 512 \times 559$ voxels, $0.726 \times 0.726 \times 1$ mm^3 of voxel size) was acquired in a CT scanner, with 120 kVp. Another CT of the applicator provided the 3D coordinates of the markers. To recreate the scenario of the treatment the resected phantom with the IOERT applicator was acquired with a C-arm system which has a flat panel detector with 400×400 mm2 active surface of 0.38×0.38 mm^2 pixel size. 15 C-arm projections were acquired with relative angular distances of about 10°.
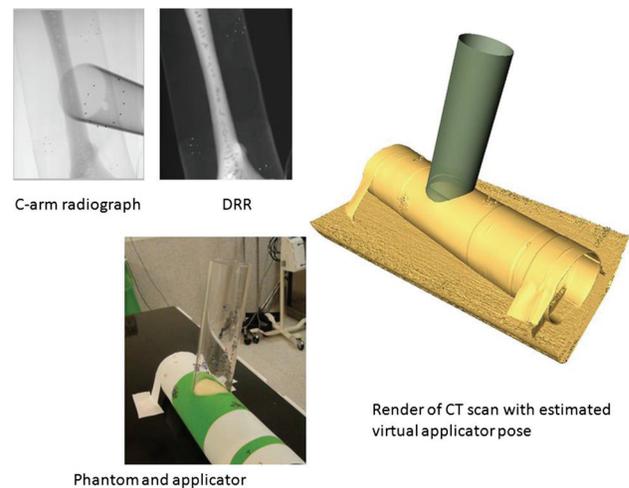
Fig. 1 C-arm projections with the applicator located in the treatment position

Following the workflow, we used one projection to find out the pose of the camera model. To make the experiment more realistic, the skin markers sets were moved ±10 mm in random directions. For each random movement experiment two estimations were computed using two different pairs of views. The final transformation found allowed to locate the virtual applicator on the pre-operative CT volume and to measure the estimated target registration error (TRE) considering the CT segmented markers' center as the ground truth.

The workflow was implemented using a custom software and [3] was used as development framework.

Results

The proposed workflow successfully and almost accurately estimated the pose of the C-arm and the initial transformation based on the skin markers (with an estimated error under 1 mm). Considering the random movements the initial TRE was in the range of 3–7 mm and after the intensity-based registration step the maximum TRE improvement achieved was 4 mm.

Conclusions

We have proposed a new workflow to supervise IOERT treatment planning including C-arm intra-operative images to estimate the applicator pose relative to the patient position in the actual scenarios. The proposed workflow has been tested in a phantom experiment.

Results show that the workflow could allow a correct repositioning even when displacements of around 10 mm and 10° are present.

References

[1] García-Vázquez, V., et al. (2013). "Feasibility of integrating a multi-camera optical tracking system in intra-operative electron radiation therapy scenarios." Physics in Medicine and Biology 58(24): 8769.

[2] Kneip, L., et al. (2011). A novel parametrization of the perspective-three-point problem for a direct computation of absolute camera position and orientation. Computer Vision and Pattern Recognition (CVPR), 2011 IEEE Conference on, IEEE.

[3] G. Wollny, P. Kellman, M.-J. Ledesma-Carbayo, M. M. Skinner, J.-J. Hublin, Th. Hierl, MIA - A Free and Open Source Software for Gray Scale Medical Image Analysis, Source Code for Biology and Medicine, 2013, 8:20

Chest bone registration using weighted-demons in serial CT scans

J. Oh[1], J. Lee[1], G. Kim[1], M. Cheon[1], Y. Park[1]
[1]DMC R&D Center, Samsung Electronics, Suwon, Korea

Purpose

For a precise longitudinal assessment of bone metastases in the ribs and spine, registration of the chest bone in serial chest computed tomography (CT) scans is a prerequisite. Not only rigid registration, but deformable registration is also necessary because of non-rigid motion of the chest bone by breathing, but is challenging. It is due to a variation in the inflate phase at scan time between baseline and follow-up scans, and different movement profile in the far interior and exterior regions of the chest bone. Thus, existing approaches based on equivalent contribution of intensity in the image domain to registration cannot produce correct alignment in the bone region. To address this issue, we propose a straightforward approach to registering a target region selectively using a modified version of Demons algorithm with high speed.

Methods

The chest bone is first segmented using its high CT density value and followed by morphology operations. For rigidly registering the baseline and follow-up scans, the 3-D coordinates of the uniformly sampled points on the segmented bone are utilized in the iterative closest point (ICP) algorithm [1] and it estimates suboptimal rotation and translation matrices to best match the two clouds of points.

To correct for the remaining deformable motion error, a modified version of Demons is used. In contrast to the original Demons, introduced by Thirion [2], the weighted-Demons proposed utilizes a new dissimilarity measure which is referred to as a sum of Gaussian-weighted squared difference. It is characterized as weighting the demons' forces on the target region but also taking into account the surroundings with gradually decreasing strength adjusted by the Gaussian kernel. The inputs in the weighted-Demons algorithm are static and moving images, and their binary masks representing the target region of interest in each image. And to determine the weighting degree over the image domain, a Gaussian-weighted distance map from the closest nonzero value in the binary mask is computed. In accordance with the new dissimilarity measure, the velocity field is analytically derived in the bi-directional format [3, 4], which consists of active and passive forces, of the Demons algorithm for algorithmic acceleration. The velocity field is then accrued to the displacement field as iteration goes. Accordingly, the moving image and its binary mask are deformed to be matched. To offset the degrading effect occurred by warping the moving image only, which may cause subtraction errors in quantifying bone metastases, the symmetric registration framework was employed such that a half of transformation is applied to the moving image whereas a half of inverse transformation is applied to the fixed image.

Results

To validate the performance of the weighted-Demons algorithm, serial chest CT scans of 24 patients were used for tests. The serial CT scans are mostly scanned in 2.5 mm helical CT machine from a variety of manufacturers and consist of baseline and follow-up scans with a gap of at least 6 months. It is observed that the chest bone has different motion profile in surroundings in that the far exterior region including attached muscles moves toward the superior direction while the far interior region including soft organ tissues such as the liver moves toward the inferior direction. In the test, the parameters, alpha and Gaussian standard deviation for smoothing the velocity field, displacement field, and Gaussian-weighting are 0.5, 3 mm, 3 mm, and 6 mm, respectively. Figure 1 shows a visual comparison of registration results in axial slices between Demons and weighted Demons, where Demons algorithm yields large mismatching error in the shoulder bone and spine whereas weighted-Demons algorithm does not. Figure 2 demonstrates the overlap of registered bones in 3-D, where weighted-Demons achieves higher matching performance in scapula and lower ribs regions. The scapula is more susceptible to misalignment because registration is performed as a whole to the torso, but not separately to the scapula. Also, the lower ribs are prone to misalignment due to large motion of the liver nearby. In the dice similarity coefficient (DSC) measurement, as a matching rate between registered two bone volumes, the weighted Demons with an average of 93 ± 1.5 % outperformed the Demons algorithm with an average of 88 ± 2 %. We implemented this algorithm in C++ in parallel with the aid of a graphics card of nVIDIA GTX 680 in Intel i7, 3.5 GHz and achieved computation time of 143 s to complete registration for 1 patient.
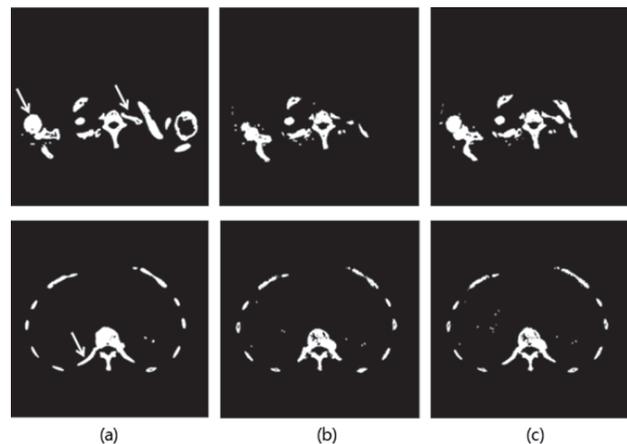
Fig. 1 A visual comparison of registration results for 2 axial slices; **a** baseline, **b** registered follow-up using Demons, **c** registered follow-up using w-Demons. Note the regions highlighted with *white arrow*
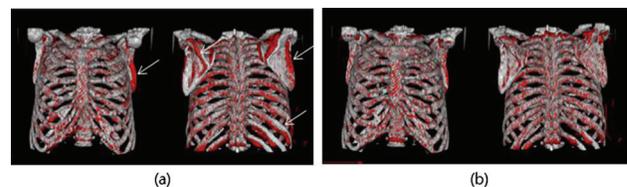
Fig. 2 A volume rendering comparison of registration results using **a** Demons and **b** w-Demons. *White one* is a baseline and *red one* is a registered follow-up. Note the *white arrow* indicating the difference